Geophysical Research Letters

RESEARCH LETTER
10.1029/2018GL078312

Key Points:
- Most of the drying over the U.S. Southwest from 1983 to 2012 is driven by internal variability rather than anthropogenic climate change
- Removing the effects of atmospheric circulation variability largely reconciles drying trends in observations and climate model simulations
- Prospects and limitations for the detection of forced temperature and precipitation trends in observations are discussed

Supporting Information:
- Supporting Information S1

Correspondence to:
F. Lehner,
flehner@ucar.edu

Citation:
Lehner, F., Deser, C., Simpson, I. R., & Terray, L. (2018). Attributing the U.S. Southwest's recent shift into drier conditions. *Geophysical Research Letters*, *45*, 6251–6261. https://doi.org/10.1029/2018GL078312

Received 11 APR 2018
Accepted 1 JUN 2018
Accepted article online 8 JUN 2018
Published online 29 JUN 2018

Attributing the U.S. Southwest's Recent Shift Into Drier Conditions

Flavio Lehner[1], Clara Deser[1], Isla R. Simpson[1], and Laurent Terray[2]

[1]National Center for Atmospheric Research, Climate and Global Dynamics Laboratory, Boulder, CO, USA, [2]Université de Toulouse, CERFACS/CNRS, Climate, Environment, Coupling and Uncertainties Group, Toulouse, France

Abstract The U.S. Southwest experienced a strong hydroclimate trend from the 1980s to the 2010s, from cool and wet to warm and dry conditions. Attribution of this trend is challenging due to the influence of internal variability but desired by water managers eager to plan for robust signals of climate change in this water-scarce region. Here we use an empirical method based on constructed circulation analogues to assess the contribution of atmospheric circulation variability to the recent observed hydroclimate trend. Consistent with other studies, we find the observed precipitation trend from 1983 to 2012 to be mainly due to internal atmospheric circulation variability that is driven in part by decadal-scale tropical Pacific sea surface temperature changes. Removing this internal dynamical component brings the observed precipitation trend into closer agreement with the anthropogenically forced response in climate models, demonstrating progress toward an integrated perspective on climate change attribution.

Plain Language Summary The U.S. Southwest has been getting drier and warmer over the last few decades. These changes fit the common narrative of what might be expected to happen in response to increasing greenhouse gas concentrations. However, natural variability of precipitation and temperature is known to be large in this region, making it difficult to clearly attribute the recent drying and warming to greenhouse gas forcing. Here we show that while the warming is largely due to greenhouse gas forcing, the drying is mostly due to internal climate variability. To date, only an insignificant drying remains after accounting for this internal climate variability. Unlike previous studies that relied exclusively on climate models, we are able to reach these conclusions based on a combination of observations, an empirical statistical method, and climate models.

1. Introduction

Recent decades have seen strong hydroclimate trends over the United States (U.S.) Southwest (SW), from relatively wetter and colder conditions in the 1980s to relatively drier and warmer conditions in the 2000s and beyond (Seager & Hoerling, 2014). Intermittent drought conditions and below average streamflow from the early 2000s onward have challenged water management and prompted water agencies to develop new strategies for drought mitigation (Bureau of Reclamation, 2014; Raff et al., 2013). A critical question is to what extent are recent trends due to internal variability as opposed to anthropogenic climate change and thus to what extent are such trends expected to continue? This question is motivated by the potential for future hydroclimate variability to be outside of the historical envelope (Cook et al., 2015), which might require fundamentally different water resource management and infrastructure.

Climate models robustly project an expansion of the subtropics with warming (Held & Soden, 2006). This expansion is often implicated in observed drying trends over subtropical to midlatitude regions (e.g., Prein et al., 2016) but to date remains difficult to actually detect and attribute in observations (Davis & Rosenlof, 2012). Also, the expansion is not necessarily expected to manifest itself over land in the form of circulation-driven precipitation declines, especially over the U.S. SW (Greve et al., 2014; He & Soden, 2016a; Schmidt & Grise, 2017). Rather, a thermodynamically driven decrease in mean moisture convergence during the warm season seems to dominate the projected drying there (Ting et al., 2018). Projected increases in winter precipitation may partially mitigate this drying trend but only along the U.S. West Coast (Seager et al., 2014; Simpson et al., 2016).

At least two robust arguments emerge from the literature on the topic of the U.S. SW's recent shift into drier conditions: (1) the precipitation shift is not primarily forced by anthropogenic increases in greenhouse gas (GHG) concentrations; instead, it is mainly a result of internal decadal climate variability, in particular a shift

from the positive to the negative phase of the Pacific Decadal Oscillation (PDO) and ensuing teleconnections to North America (Delworth et al., 2015; Hoerling et al., 2010; Schubert et al., 2009; Seager et al., 2005; Seager & Ting, 2017; Zhao et al., 2017); (2) the hydrologic impact of this shift is exaggerated by anthropogenic warming, affecting various aspects of hydroclimate, such as increased evaporative demand leading to elevated drought risk (Diffenbaugh et al., 2015; Lehner, Coats, et al., 2017), lower streamflow (McCabe et al., 2017; Vano et al., 2012; Woodhouse et al., 2016), lower runoff efficiency (Lehner, Wahl, et al., 2017), reduced snowpack (Mote et al., 2005), and altered seasonality of hydrographs (Clow, 2010).

Despite the broad consensus on the relative roles of internal variability and anthropogenic forcing, the exact quantification of the individual factors contributing to the U.S. SW's recent shift into drier conditions remains challenging (Schubert et al., 2016). For example, it seems likely that tropical sea surface temperatures (SSTs) during recent decades were influenced to some extent by GHG forcing (e.g., Park et al., 2017), although the spatial fingerprint of GHG forcing on tropical SSTs and precipitation appears distinct from the observed trend over recent decades (Deser & Phillips, 2009). Further, uncertainties remain with regard to observed SST trends (Coats & Karnauskas, 2017; Deser et al., 2010). It is possible that GHG forcing amplifies Pacific decadal variability itself (Liguori & Di Lorenzo, 2018), in turn affecting hydroclimate variability. More generally, we expect precipitation variability to increase more robustly with warming than mean precipitation over much of the globe, including the U.S. SW (Pendergrass et al., 2017). Finally, recent studies have suggested an influence of Arctic sea ice loss on midlatitude precipitation (Blackport & Kushner, 2017; Cvijanovic et al., 2017; Deser, Sun, et al., 2016; Lee et al., 2015; Swain et al., 2017; Wang et al., 2018), although such an influence might be partially offset by opposing climate change effects (Barnes & Screen, 2015; Deser et al., 2015; Harvey et al., 2014).

Importantly, most previous studies have relied on model simulations to attribute recent hydroclimate trends to either forced or internal components of climate change. Such simulations are capable of reproducing observed hydroclimate trends when forced with observed SSTs in so-called Atmospheric Model Intercomparison Project (AMIP) modeling experiments (e.g., Hoerling et al., 2010). However, historical simulations with coupled models struggle to reproduce observed hydroclimate trends, due to biases in temporal variability and spatial gradients of SSTs (Kajtar et al., 2018; Luo et al., 2018; Seager & Vecchi, 2010; Shin & Sardeshmukh, 2011; van Haren et al., 2013). It is thus desirable to approach the attribution of recent U.S. SW hydroclimate trends from both a modeling *and* observational perspective and investigate the degree of consistency that can be achieved from the two information sources.

A promising technique to achieve such comparability is "dynamical adjustment", in which the effects of atmospheric circulation variability on surface climate are removed. The residual variability then reveals the internal and anthropogenically forced thermodynamic signal, absent any forced changes in circulation (Cattiaux et al., 2012; Wallace et al., 2012). New methods of dynamical adjustment based on constructed circulation analogues (CCAs), partial least squares regression, and self-organizing maps have recently been used to estimate the importance of internal atmospheric circulation variability for Northern Hemisphere temperature (Deser, Terray, & Phillips, 2016; Horton et al., 2015; Lehner, Deser, & Terray, 2017; O'Reilly et al., 2017; Smoliak et al., 2015), land-atmosphere coupling during summer (Merrifield et al., 2017), and dissection of model biases in future precipitation projections (Fereday et al., 2017).

Here we use a CCA technique to remove the influence of atmospheric circulation variability from observed precipitation and temperature anomalies to attribute underlying trends over the U.S. SW. In addition, we use a set of climate model simulations to assess the relative influence of GHG forcing and internal variability on the observed trends. We focus on the 30-year trend from 1983 to 2012, a common time period between observations and available model simulations.

2. Materials and Methods

2.1. Observational Data Sets

We use the 1° × 1° gridded Global Precipitation Climatology Centre (GPCC) data set (Schneider et al., 2015) from 1901 to 2015 and the 1° × 1° gridded Berkeley Earth Surface Temperature (BEST) data set (Rohde et al., 2013) from 1901 to 2015. In addition, we use a 1/8° × 1/8° gridded 100-member observational "ensemble" data set of precipitation and temperature from 1980 to 2012, which reflects uncertainty from various

station data processing steps (Newman et al., 2015). All precipitation trends are expressed as percent deviations from their 1981–2010 mean. We use gridded sea level pressure (SLP) from the 2° × 2° Twentieth Century Reanalysis version 2c from 1901 to 2014 (Compo et al., 2011) after regridding bilinearly to 1° × 1°. The SLP data are extended through 2015 with ERA-Interim (Dee et al., 2011) as described in Lehner, Deser, et al. (2017). All data are monthly means.

2.2. Dynamical Adjustment Technique

We use a CCA-based dynamical adjustment technique to remove atmospheric circulation variability from observed precipitation (GPCC) and surface air temperature (SAT; BEST). The empirical technique is described in detail in Deser, Terray, and Phillips (2016) and summarized here. For each month, for example, January 2012, the SLP patterns from all other available Januaries are pooled (domain: 20N°–90°N, 180W°–10°W). Out of these 114 SLP patterns, 100 are randomly sampled and combined in a linearly optimal way to form a constructed SLP analogue that resembles most closely the SLP pattern for the month in question. The coefficients derived from the optimal linear combination of SLP patterns are then applied to the corresponding precipitation and SAT to form the "dynamically induced" portion of the precipitation and SAT field. The procedure of randomly selecting 100 SLP patterns is repeated 100 times with replacement to guard against overfitting. The final CCA and accompanying dynamically induced precipitation and SAT are the average over those 100 iterations. The dynamically induced portion is then subtracted from the original precipitation and SAT field to obtain the "dynamically adjusted" portion. Prior to selecting the SLP patterns and constructing the analogues, precipitation, SAT, and SLP are detrended for each grid cell and calendar month by removing an estimate of the forced response of that variable (see section S1 and Figure S1 in the supporting information for more details).

2.3. Model Simulations

We use monthly mean output from a set of climate model simulations (Table S1). First, we use 10-member ensembles of atmosphere-only simulations with observed SSTs prescribed globally from the Community Earth System Model version 1 (CESM) and Geophysical Fluid Dynamics Laboratory CM2.1 (GFDL). These simulations are termed Global Ocean Global Atmosphere (GOGA). For CESM, we also use a 10-member ensemble in which observed SSTs are only prescribed in the tropics (28°S–28°N), with climatological SSTs and sea ice outside 35° latitude, and a linear interpolation in between, termed Tropical Ocean Global Atmosphere (TOGA).

Second, we use fully coupled simulations from the Coupled Model Intercomparison Project Phase 5 (Taylor et al., 2012; 40 models, one simulation each) and large ensembles of fully coupled simulations with CESM (40 simulations; CESM LE) and GFDL (10 simulations; GFDL LE). The *historical* and *rcp85* portions of these ensembles are merged at years 2005/2006.

Third, we use a 2,200-year long preindustrial control simulation with CESM and a 2,600-year long simulation with the atmospheric component of CESM, the Community Atmosphere Model 5 (hereafter CESM atmosphere only). The latter simulation has prescribed climatological SSTs that were derived from the aforementioned preindustrial control simulation and hence excludes any interannual to decadal SST variability such as El Niño–Southern Oscillation or PDO.

The GOGA and TOGA simulations are used to test whether climate models are able to simulate the observed hydroclimate trends when given the observed lower boundary conditions over the oceans together with realistic historical radiative forcing. The fully coupled simulations are used to investigate how much of the observed hydroclimate trends can potentially be attributed to anthropogenic forcing and whether coupled models are generally able to produce hydroclimate variability of the same magnitude as observed.

3. Results

3.1. Precipitation Trend 1983–2012

The observed water year precipitation trend from 1983 to 2012 (i.e., October–September 1982/1983 to October–September 2011/2012) over the U.S. SW features widespread drying, with the most pronounced drying ($>$50% 30 years^{-1}) in the southern parts of Arizona and New Mexico (Figure 1a). The drying pattern encompasses most of the Colorado River and Rio Grande basins, two of the most important rivers in the U.S. SW, which consequentially saw significant depletion of water resources over this time period.

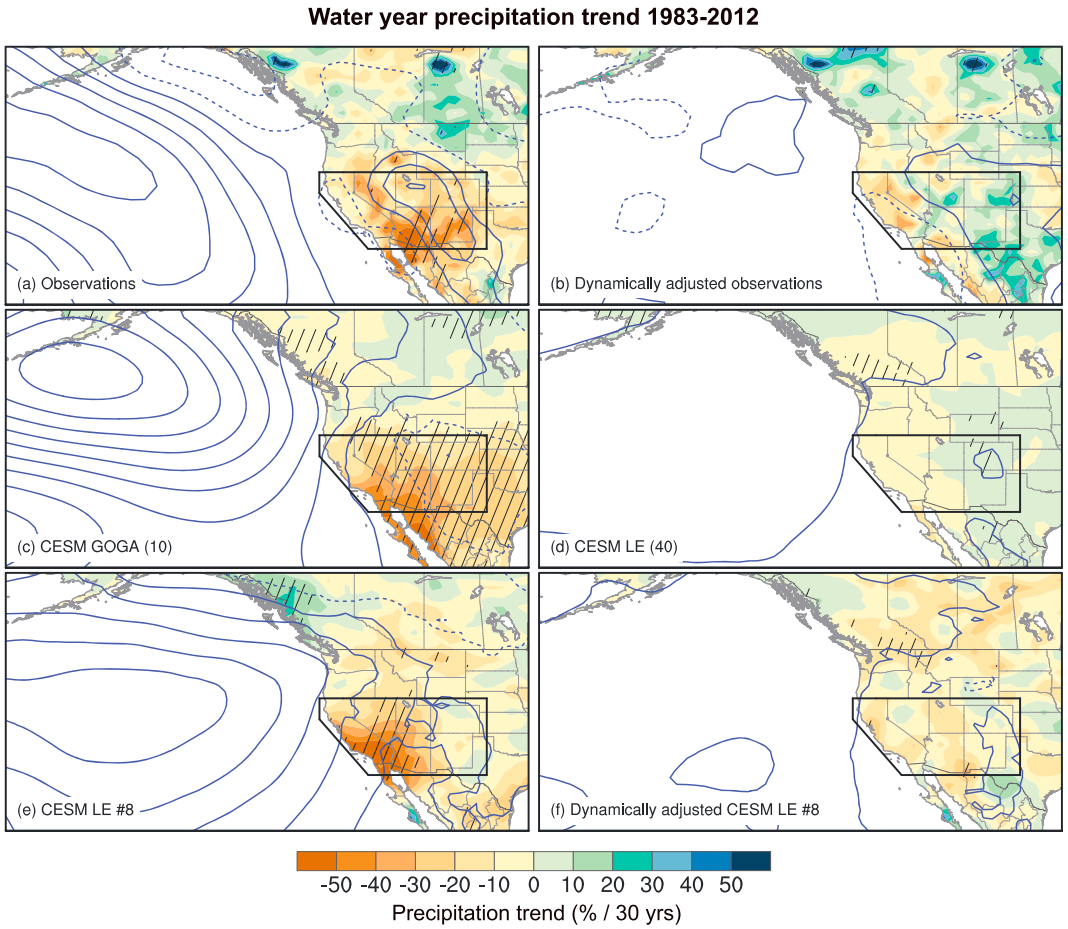

Figure 1. Water year precipitation trend from 1983 to 2012 in (a) observations, (b) dynamically adjusted observations, (c) CESM GOGA ensemble mean, (d) CESM LE mean, (e) CESM LE member #8, and (f) dynamically adjusted CESM LE member #8, expressed as percent of the respective 1981–2010 mean. Hatching indicates significant trends (95% confidence). Contours are sea level pressure trend in 0.5 hPa 30 years^{-1} increments starting at ±0.25 hPa. Number of simulations of each ensemble is given in brackets. CESM = Community Earth System Model; GOGA = Global Ocean Global Atmosphere.

Can the precipitation trend be attributed to an anomalous atmospheric circulation trend? The SLP trend field indicates a strong ridge over the North Pacific as well as a weaker ridge over the U.S. SW, suggestive of a dynamical contribution to the dry conditions. After dynamically adjusting the precipitation observations, most of the drying is eliminated (Figure 1b). The lack of appreciable trends in the residual SLP trend field indicates that the CCA method accounts for nearly all of the observed atmospheric circulation trend.

Can the observed atmospheric circulation trend be attributed to the observed SST trend pattern? Indeed, much of the observed precipitation and SLP trend pattern is recovered by the ensemble mean of the CESM GOGA simulations (Figure 1c), suggesting a governing influence of SSTs for observed hydroclimate. Note, however, that the simulated SLP trend pattern over Canada and the western United States is inconsistent with observations and leads to an underestimation of wetting there. These inconsistencies are present to some degree in all 10 of the individual GOGA ensemble members (not shown), suggesting there is a systematic error in the model's response to the prescribed SSTs, rather than this being a feature of internal atmospheric variability. It is worth noting that the positive SLP trend over the U.S. Interior West is less robust across observational data sets than the large-scale ridge over the North Pacific and could thus be related to difficulties with estimating SLP over sparsely observed and mountainous areas (Figure S2). Like CESM, GFDL GOGA reproduces the large-scale SLP trend pattern but not the smaller features over the continent. However, GFDL GOGA does not simulate the observed drying pattern as well as CESM GOGA (Figure S3).

Can the observed atmospheric circulation trend, and by extension the observed SST trend pattern, be attributed to anthropogenic forcing? The CESM LE mean represents an estimate of the forced anthropogenic response and can be used to answer this question, conditional on the forcing and the model's forced response being correct. The forced SLP trend is near zero (Figure 1d), which means we cannot attribute the observed atmospheric circulation trend to anthropogenic forcing according to CESM, nor according to other models (Figure S3). The forced SST trend pattern does not resemble the observed pattern (Figures S4b and S4d) and thus, to first order, cannot be implicated as a dominant driver of the SST trend pattern and the associated SLP and precipitation response. Rather, the observed SST trend pattern resembles the PDO, displaying similarities with the previous large PDO switch in 1936–1965 (including its SLP and precipitation response), which occurred in the absence of strong GHG forcing (Figures S4a and S4c).

Thus, assuming that most of the observed drying trend is driven by atmospheric circulation variability forced by SSTs, and that the SST trend pattern itself is not *primarily* an expression of anthropogenic forcing but an expression of internal ocean-atmosphere dynamics, we expect the dynamically adjusted observed precipitation trend to more closely resemble the forced precipitation trend from models than the unadjusted trend. Indeed, the dynamically adjusted observed precipitation trend pattern shows good agreement with the CESM LE ensemble mean trend, although some differences remain (compare Figures 1d and 1b). In particular, the dynamically adjusted observations show drying along the U.S. West Coast and western Nevada, and wetting of much of the U.S. Interior West, Texas, and eastern Mexico (Figure 1b). These residual precipitation trends are opposite in sign and generally weaker than the unadjusted trends. The patchiness of the dynamically adjusted observations compared to the smoother CESM LE ensemble mean likely reflects imperfections of the empirical CCA method due to the limited sample of SLP analogues, observational uncertainty, and additional influences not directly related to circulation.

The degree of agreement achievable through dynamical adjustment between a single climate realization and the forced response can be illustrated using the CESM LE. We apply dynamical adjustment to CESM LE member #8 (see section S1 for details), which by chance shows a drying trend that resembles observations (Figure 1e). As in observations, dynamical adjustment eliminates most of the drying and SLP trend (Figure 1f), and while the residual precipitation trend comes closer to the forced response some differences remain (compare Figures 1f and 1d). To assess the efficacy of dynamical adjustment more generally, Figure S5a shows the distribution of precipitation trends averaged over the U.S. SW region (box in Figure 1) before and after dynamical adjustment for all 40 members of CESM LE as well as observations. Dynamical adjustment narrows the distribution of trends by about 50%, with all members falling within the range −12.5 to +7.5% 30 years^{-1}. Importantly, the observed trend, which lies at the lower end of (but within) the model range before dynamical adjustment, falls near the middle of the model's distribution after dynamical adjustment: that is, near the model's forced response. This confirms that dynamical adjustment can help to reveal the forced response in the U.S. SW over this time period in observations.

3.2. Temperature Trend 1983–2012

The observed water year SAT trend is positive over much of the western United States and Canada, with largest values over the south-central United States and smallest amplitudes over south-central Canada (Figure 2a). Dynamical adjustment produces a more spatially uniform pattern of warming by reducing the magnitudes over the south-central United States and increasing them over southwestern Canada (Figure 2b). Anthropogenic GHG forcing, as represented by the CESM LE mean, can account for the general warming trend in the dynamically adjusted observations, albeit with slightly larger magnitudes (compare Figures 2d and 2b). Consequently, the unadjusted and dynamically adjusted observations, averaged over the U.S. SW, fall in the lower half of (but within) the respective ranges of CESM LE (Figure S5b). The efficacy of dynamical adjustment is again confirmed by using CESM member #8 (Figure 2e), which resembles the CESM forced response after dynamical adjustment (compare Figures 2f and 2d).

The CESM GOGA simulations reproduce the amplified (dampened) warming over the south-central United States (southern Canada) relative to the ensemble mean of CESM LE (compare Figures 2c and 2d). However, both the amplification and damping signal are overestimated significantly in CESM GOGA, leading to warming of >2 °C 30 years^{-1} over the U.S. SW and even cooling over southern Canada. The same holds true for GFDL GOGA (Figure S3). The anomalous atmospheric circulation, attributable to the observed SST

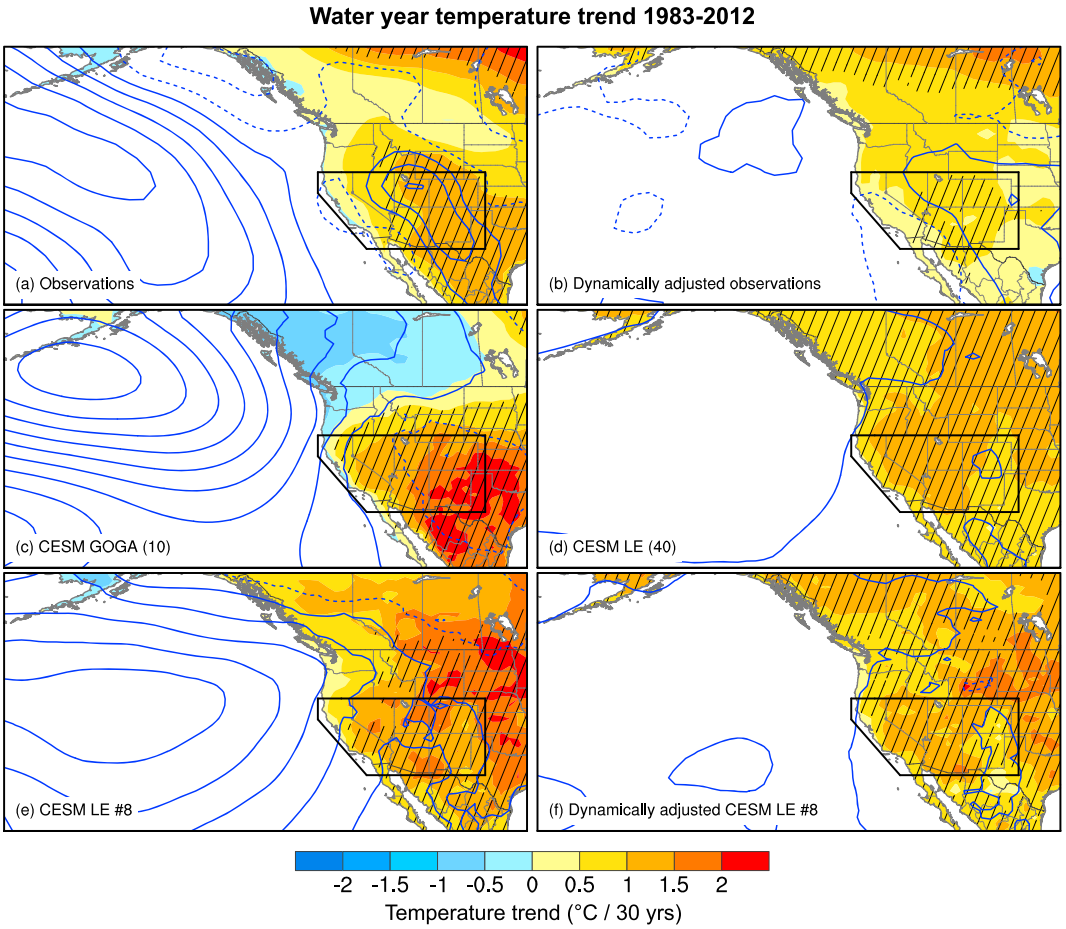

Figure 2. Same as Figure 1 but for surface air temperature. CESM = Community Earth System Model; GOGA = Global Ocean Global Atmosphere.

evolution (section 3.1), extends too far over land in the GOGA simulations, causing some of the overestimated SAT response.

The results from Figures 1 and 2 illustrate that while the models are able to recover the general precipitation and SAT features of the teleconnections originating from anomalous SSTs, the magnitude and spatial details might not be replicated exactly or might even be biased systematically**.**

3.3. Uncertainty and Seasonality of 1983–2012 Trends

The observed water year precipitation trend from GPCC, averaged over the U.S. SW region, is -19.3% 30 years^{-1} (Figure 3 and Table S2). A range of possible water year precipitation trends as derived from the observational ensemble by Newman et al. (2015) is given in gray shading in Figure 3 and illustrates the considerable observational uncertainty, spanning -21.4% 30 years^{-1} to -12% 30 years^{-1} (Figure 3a and Table S2). The dynamically adjusted water year precipitation trend is -6.1% 30 years^{-1}, which is close to zero within the methodological uncertainties, estimated here from the different detrending methods tested (red shading in Figure 3; see section S1 for details).

The water year precipitation trend is composed of drying in all seasons October–December, January–March, April–June, and July–September (Figures 3b–3e). In all seasons, dynamical adjustment reduces or reverses the negative precipitation trend to approximately zero within observational and methodological uncertainty. The Newman et al. (2015) uncertainty data are only shown for unadjusted trends; its short record does not allow us to use it in the CCA method. However, we do not expect the observational uncertainty to be affected significantly by dynamical adjustment.

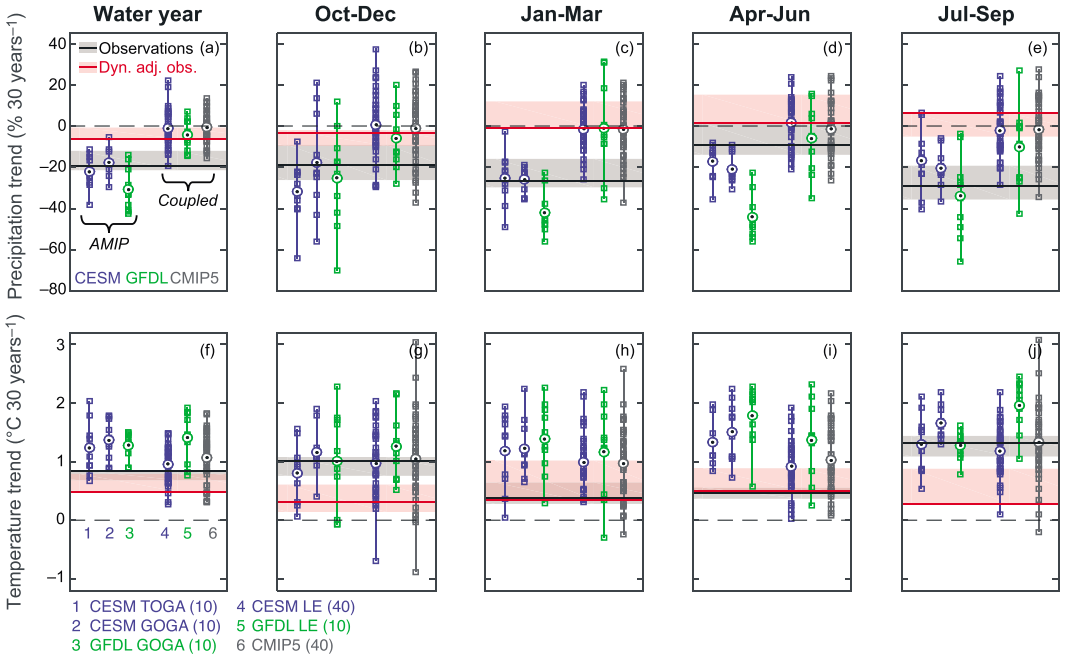

Figure 3. The 1983–2012 trends of (a–e) precipitation and (f–j) surface air temperature over the U.S. Southwest from observations and various model simulations. Black horizontal lines and gray shading indicate observations (GPCC and BEST) and observational uncertainty (Newman et al., 2015). Red horizontal lines and pink shading indicate dynamically adjusted observations and its methodological uncertainty (see section S1 for details). The individual model simulations are given as squares; each ensemble's mean is given with a circle. CESM = Community Earth System Model; GOGA = Global Ocean Global Atmosphere; GPCC = Global Precipitation Climatology Centre; BEST = Berkeley Earth Surface Temperature; TOGA = Tropical Ocean Global Atmosphere; GFDL = Geophysical Fluid Dynamics Laboratory; CMIP5 = Coupled Model Intercomparison Project Phase 5; AMIP = Atmospheric Model Intercomparison Project.

The ensemble mean precipitation trends in the coupled models are statistically indistinguishable from zero in all seasons (Figures 3a–3e). The spread of these ensembles encompasses the observed drying trend, suggesting that the coupled models are generally able to produce precipitation trends of the magnitude that has been observed from 1983 to 2012. However, it is also clear that the same models, when run with prescribed observed SSTs (GOGA), produce stronger precipitation trends than any that occur in the coupled model version (compare the most negative values for GOGA and LE simulations in Figures 3a–3e). Investigation of all possible 30-year precipitation trends (not just 1983–2012) reveals that CESM GOGA simulations generally produce stronger trends, positive and negative, than occur in any of CESM LE, CESM preindustrial control simulation, and CESM atmosphere-only control simulation (Figure S6). This occurs despite an order of magnitude smaller sample size in CESM GOGA (a total of 1,060 30-year trends in CESM GOGA and >10,000 30-year trends in the CESM coupled and atmosphere-only simulations) and is hence a robust result. It is thus conceivable that observed precipitation trends stronger than 1983–2012 would not be reproduced by coupled models but could be simulated in a GOGA setup. This illustrates the ongoing challenge for coupled models to reproduce the fidelity of observed hydroclimate variability (He & Soden, 2016b; Seager & Hoerling, 2014). GFDL GOGA simulations generally show stronger drying trends than CESM and overestimate the observed trend in April–June.

We also found that the CESM atmosphere-only control simulation produces trends as strong as observed during 1983–2012, including similar SLP and precipitation trend patterns (Figures S7a and S7b). Thus, the particular SST pattern during that period cannot be considered a necessary condition for the drying trend over the U.S. SW, in line with studies on tropical SST forcing of atmospheric ridging in the context of the recent California drought (Seager & Henderson, 2016; Teng & Branstator, 2017). However, the fact that all GOGA simulations produce a drying indicates that the chances for drying are greatly increased in the presence of the particular 1983–2012 SST trend pattern.

Finally, we investigate a 10-member ensemble of TOGA simulations with CESM (first blue boxplot in each panel of Figure 3). The TOGA and GOGA ensembles are not statistically different in the precipitation trends; they induce over the U.S. SW during 1983–2012 (Figures 3a–3e). This suggests that the extratropical SSTs were less important in bringing about the full precipitation trend over the U.S. SW, in agreement with earlier results on the relative roles of tropical and extratropical SSTs for drought over North America (Seager et al., 2005).

For SAT averaged over the U.S. SW, the observed water year trend is 0.84 °C 30 years^{-1} (0.68 to 0.85 observational uncertainty range) and the dynamically adjusted trend is 0.49 °C 30 years^{-1} (Figure 3f and Table S2). Broadly similar trends exist during individual seasons (Figures 3g–3j). Contrary to precipitation, the observed SAT trends are mostly consistent with coupled models forced with GHG increase (Figures 3f–3j). Consequently, the effect of dynamical adjustment on the observed SAT trends is smaller than that for precipitation and never leads to a cancelation or reversal of the positive trend of the observations, except in October–December when some of the dynamical adjustment methods reduce the SAT trend to almost zero.

As hinted at in Figure 2, the GOGA simulations tend to overestimate the warming trend over the SW United States, especially in spring (Figure 3i). Since the coupled models always encompass the observed SAT trend and hence show no clear sign of bias in that regard, this indicates that the SAT response to the prescribed SSTs in the GOGA simulations is likely overestimated.

4. Summary and Conclusions

Using a dynamical adjustment method, we provide evidence for the importance of atmospheric circulation variability for the strong drying and warming trend over the U.S. SW from 1983 to 2012. Critically, the method is based on observations alone. After applying dynamical adjustment, closer correspondence emerges between the residual precipitation trend and the anthropogenically forced precipitation trend pattern given by climate models. Using model simulations with prescribed observed SSTs, we show that the anomalous atmospheric circulation that caused the negative precipitation trend can be attributed with high probability to teleconnections arising from tropical Pacific SSTs.

Our approach provides a novel attribution perspective on U.S. SW precipitation trends that combines both observations and models. In particular, dynamical adjustment enables progress toward the long-elusive detection of forced precipitation trends in observations in situations where thermodynamically forced trends have arisen alongside influences of internal atmospheric circulation variability (Hegerl et al., 2015). However, more sensitivity tests over other regions and time periods, such as the exceptional drought conditions over California from 2012 to 2016, are planned to confirm the utility of the dynamical adjustment method for precipitation.

While different models agree on the general precipitation and temperature response to prescribed SSTs, as well as GHG forcing, there remain considerable differences in the magnitude of those responses. This makes it difficult to exactly quantify the relative roles of GHG, internal atmospheric variability, and atmospheric variability forced by SSTs in the observed trends. We also show notable uncertainties in the observed trends themselves, something that poses a challenge for model evaluation (Deser et al., 2017, 2018).

Coupled models do not suggest a dominant influence of GHGs on the observed 1983–2012 Pacific SST trend pattern. However, these models contain biases in tropical SSTs and precipitation, undermining confidence in the corresponding model-projected forced responses—which in turn could affect U.S. SW precipitation through teleconnections. Further, dry conditions have prevailed in parts of the U.S. SW even after 2012, despite a string of positive PDO years since 2013, inviting speculation as to whether the emergence of a forced drying trend is imminent (Seager et al., 2007). Our observed record of SSTs over the last century does, however, indicate that similar magnitude SST and precipitation trends have occurred in the past under very different anthropogenic forcing, indicating that natural variability is capable of contributing the dominant fraction of the trends discussed here.

While much of the drought conditions over the U.S. SW since the 2000s were caused by the precipitation deficit, the accompanying warming helped to deepen the drought through increased evapotranspiration (Weiss et al., 2009). Unlike the precipitation deficit, this warming is driven primarily by anthropogenic forcing from GHGs rather than atmospheric circulation variability (although some amplification might be attributable

to the particular 1983–2012 SST evolution). Thus, it is important to distinguish between forced and internal aspects of the recent droughts (e.g., Williams et al., 2015). In this case, drying and warming combined to form what in some regions equates to one of the steepest hydroclimate trends of the last several centuries (Lehner, Wahl, et al., 2017). While precipitation will continue to show significant interannual to decadal variability over the U.S. SW, it will likely do so over a rising background temperature, which in turn will increase the probability of drought whenever precipitation deficits occur (Udall & Overpeck, 2017; Woodhouse et al., 2010).

Predictability of decadal hydroclimate trends over the U.S. SW, such as the one from 1983 to 2012, remains low. State-of-the-art decadal prediction systems struggle to provide skillful forecasts of tropical Pacific SSTs beyond 2-year lead times (Yeager et al., 2018). However, 2-year La Niñas, which often induce drought conditions over the southern United States (Okumura et al., 2017), can now be successfully predicted 2 years before their onset (DiNezio, 2017). On seasonal time scales, temperature forecasts over the U.S. SW are now skillful enough that they can improve streamflow forecasts in temperature-sensitive basins such as the Colorado River or Rio Grande (Lehner, Wood, et al., 2017). Thus, with increasing influence of temperature on hydroclimate, an opportunity might arise to mitigate some of the negative impacts of such trends on water resources through better predictability of temperature relative to precipitation.

Acknowledgments

We are grateful to Sloan Coats, Pedro DiNezio, Ruixia Guo, Andrew Newman, Angeline Pendergrass, Andreas Prein, Yaga Richter, Andrew Wood, and Stephen Yeager for discussion; to Tingting Fan, Yu Kosaka, and Adam Phillips for sharing simulations and for technical support; and to two anonymous reviewers for constructive feedback. We acknowledge the efforts of all those who contributed to producing the simulations and observational data sets. All CESM simulations are available on earthsystemgrid.org; contact Yu Kosaka (ykosaka@atmos.rcast.u-tokyo.ac.jp) for the GFDL simulations. The National Center for Atmospheric Research is sponsored by the National Science Foundation. F. L. is supported by a Postdoc Applying Climate Expertise (PACE) fellowship cosponsored by the National Oceanic and Atmospheric Administration and the Bureau of Reclamation and administered by the Cooperative Programs for the Advancement of Earth System Science (CPAESS).

References

Barnes, E. A., & Screen, J. A. (2015). The impact of Arctic warming on the midlatitude jet-stream: Can it? Has it? Will it? *Wiley Interdisciplinary Reviews: Climate Change*, *6*, 277–286. https://doi.org/10.1002/wcc. 337

Blackport, R., & Kushner, P. J. (2017). Isolating the atmospheric circulation response to arctic sea ice loss in the coupled climate system. *Journal of Climate*, *30*(6), 2163–2185. https://doi.org/10.1175/JCLI-D-16-0257.1

Bureau of Reclamation (2014). Climate change adaptation strategy (50 pp.). Retrieved from https://www.usbr.gov/climate/docs/ClimateChangeAdaptationStrategy.pdf

Cattiaux, J., Yiou, P., & Vautard, R. (2012). Dynamics of future seasonal temperature trends and extremes in Europe: A multi-model analysis from CMIP3. *Climate Dynamics*, *38*(9-10), 1949–1964. https://doi.org/10.1007/s00382-011-1211-1

Clow, D. W. (2010). Changes in the timing of snowmelt and streamflow in Colorado: A response to recent warming. *Journal of Climate*, *23*(9), 2293–2306. https://doi.org/10.1175/2009JCLI2951.1

Coats, S., & Karnauskas, K. B. (2017). Are simulated and observed twentieth century tropical Pacific Sea surface temperature trends significant relative to internal variability? *Geophysical Research Letters*, *44*, 9928–9937. https://doi.org/10.1002/2017GL074622

Compo, G. P., Whitaker, J. S., Sardeshmukh, P. D., Matsui, N., Allan, R. J., Yin, X., et al. (2011). The twentieth century reanalysis project. *Quarterly Journal of the Royal Meteorological Society*, *137*(654), 1–28. https://doi.org/10.1002/qj. 776

Cook, B. I., Ault, T. R., & Smerdon, J. E. (2015). Unprecedented 21st century drought risk in the American Southwest and Central Plains. *Science Advances*, *1*(1), e1400082. https://doi.org/10.1126/sciadv. 1400082

Cvijanovic, I., Santer, B. D., Bonfils, C., Lucas, D. D., Chiang, J. C. H., & Zimmerman, S. (2017). Future loss of Arctic sea-ice cover could drive a substantial decrease in California's rainfall. *Nature Communications*, *8*(1), 1947–1911. https://doi.org/10.1038/s41467-017-01907-4

Davis, S. M., & Rosenlof, K. H. (2012). A multidiagnostic intercomparison of tropical-width time series using reanalyses and satellite observations. *Journal of Climate*, *25*(4), 1061–1078. https://doi.org/10.1175/JCLI-D-11-00127.1

Dee, D. P., Uppala, S. M., Simmons, A. J., Berrisford, P., Poli, P., Kobayashi, S., et al. (2011). The ERA-Interim reanalysis: Configuration and performance of the data assimilation system. *Quarterly Journal of the Royal Meteorological Society*, *137*(656), 553–597. https://doi.org/10.1002/qj. 828

Delworth, T. L., Zeng, F., Rosati, A., Vecchi, G. A., & Wittenberg, A. T. (2015). A link between the hiatus in global warming and North American drought. *Journal of Climate*, *28*(9), 3834–3845. https://doi.org/10.1175/JCLI-D-14-00616.1

Deser, C., & Phillips, A. S. (2009). Atmospheric circulation trends, 1950–2000: The relative roles of sea surface temperature forcing and direct atmospheric radiative forcing. *Journal of Climate*, *22*(2), 396–413. https://doi.org/10.1175/2008JCLI2453.1

Deser, C., Phillips, A. S., & Alexander, M. A. (2010). Twentieth century tropical sea surface temperature trends revisited. *Geophysical Research Letters*, *37*, L10701. https://doi.org/10.1029/2010GL043321

Deser, C., Simpson, I. R., McKinnon, K. A., & Phillips, A. S. (2017). The Northern Hemisphere extra-tropical atmospheric circulation response to ENSO: How well do we know it and how do we evaluate models accordingly? *Journal of Climate*, *30*(13), 5059–5082. https://doi.org/10.1175/JCLI-D-16-0844.1

Deser, C., Simpson, I. R., Phillips, A. S., & McKinnon, K. A. (2018). How well do we know ENSO's climate impacts over North America, and how do we evaluate models accordingly? *Journal of Climate*, *31*(13), 4991–5014. https://doi.org/10.1175/JCLI-D-17-0783.1

Deser, C., Sun, L., Tomas, R. A., & Screen, J. (2016). Does ocean coupling matter for the northern extratropical response to projected Arctic sea ice loss? *Geophysical Research Letters*, *43*, 2149–2157. https://doi.org/10.1002/2016GL067792

Deser, C., Terray, L., & Phillips, A. S. (2016). Forced and internal components of winter air temperature trends over North America during the past 50 years: Mechanisms and implications. *Journal of Climate*, *29*(6), 2237–2258. https://doi.org/10.1175/JCLI-D-15-0304.1

Deser, C., Tomas, R. A., & Sun, L. (2015). The role of ocean-atmosphere coupling in the zonal-mean atmospheric response to Arctic sea ice loss. *Journal of Climate*, *28*(6), 2168–2186. https://doi.org/10.1175/JCLI-D-14-00325.1

Diffenbaugh, N. S., Swain, D. L., & Touma, D. (2015). Anthropogenic warming has increased drought risk in California. *Proceedings of the National Academy of Sciences*, *112*(13), 3931–3936. https://doi.org/10.1073/pnas. 1422385112

DiNezio, P. N., Deser, C., Karspeck, A., Yeager, S., Okumura, Y., Danabasoglu, G., et al. (2017). A two-year forecast for a 60–80% chance of La Niña in 2017–18. *Geophysical Research Letters*, *44*, 11,624–11,635. https://doi.org/10.1002/2017GL074904

Fereday, D., Chadwick, R., Knight, J., & Scaife, A. A. (2017). Atmospheric dynamics is the largest source of uncertainty in future winter European rainfall. *Journal of Climate*, *31*(3), 963–977. https://doi.org/10.1175/JCLI-D-17-0048.1

Greve, P., Orlowsky, B., Mueller, B., Sheffield, J., Reichstein, M., & Seneviratne, S. I. (2014). Global assessment of trends in wetting and drying over land. *Nature Geoscience*, *7*(10), 716–721. https://doi.org/10.1038/NGEO2247

Harvey, B. J., Shaffrey, L. C., & Woollings, T. J. (2014). Equator-to-pole temperature differences and the extra-tropical storm track responses of the CMIP5 climate models. *Climate Dynamics*, *43*(5-6), 1171–1182. https://doi.org/10.1007/s00382-013-1883-9

He, J., & Soden, B. J. (2016a). A re-examination of the projected subtropical precipitation decline. *Nature Climate Change*, *7*(1), 53–57. https://doi.org/10.1038/nclimate3157

He, J., & Soden, B. J. (2016b). Does the lack of coupling in SST-forced atmosphere-only models limit their usefulness for climate change studies? *Journal of Climate*, *29*(12), 4317–4325. https://doi.org/10.1175/JCLI-D-14-00597.1

Hegerl, G. C., Black, E., Allan, R. P., Ingram, W. J., Polson, D., Trenberth, K. E., et al. (2015). Challenges in quantifying changes in the global water cycle. *Bulletin of the American Meteorological Society*, *96*(7), 1097–1115. https://doi.org/10.1175/BAMS-D-13-00212.1

Held, I. M., & Soden, B. J. (2006). Robust responses of the hydrological cycle to global warming. *Journal of Climate*, *19*(21), 5686–5699. https://doi.org/10.1175/JCLI3990.1

Hoerling, M., Eischeid, J., & Perlwitz, J. (2010). Regional precipitation trends: Distinguishing natural variability from anthropogenic forcing. *Journal of Climate*, *23*(8), 2131–2145. https://doi.org/10.1175/2009JCLI3420.1

Horton, D. E., Johnson, N. C., Singh, D., Swain, D. L., Rajaratnam, B., & Diffenbaugh, N. S. (2015). Contribution of changes in atmospheric circulation patterns to extreme temperature trends. *Nature*, *522*(7557), 465–469. https://doi.org/10.1038/nature14550

Kajtar, J. B., Santoso, A., McGregor, S., England, M. H., & Baillie, Z. (2018). Model under-representation of decadal Pacific trade wind trends and its link to tropical Atlantic bias. *Climate Dynamics*, *50*, 1471–1484. https://doi.org/10.1007/s00382-017-3699-5

Lee, M. Y., Hong, C. C., & Hsu, H. H. (2015). Compounding effects of warm sea surface temperature and reduced sea ice on the extreme circulation over the extratropical North Pacific and North America during the 2013–2014 boreal winter. *Geophysical Research Letters*, *42*, 1612–1618. https://doi.org/10.1002/2014GL062956

Lehner, F., Coats, S., Stocker, T. F., Pendergrass, A. G., Sanderson, B. M., Raible, C. C., & Smerdon, J. E. (2017). Projected drought risk in 1.5°C and 2°C warmer climates. *Geophysical Research Letters*, *44*, 7419–7428. https://doi.org/10.1002/2017GL074117

Lehner, F., Deser, C., & Terray, L. (2017). Toward a new estimate of "time of emergence" of anthropogenic warming: Insights from dynamical adjustment and a large initial-condition model ensemble. *Journal of Climate*, *30*(19), 7739–7756. https://doi.org/10.1175/JCLI-D-16-0792.1

Lehner, F., Wahl, E. R., Wood, A. W., Blatchford, D. B., & Llewellyn, D. (2017). Assessing recent declines in upper Rio Grande runoff efficiency from a paleoclimate perspective. *Geophysical Research Letters*, *44*, 4124–4133. https://doi.org/10.1002/2017GL073253

Lehner, F., Wood, A. W., Llewellyn, D., Blatchford, D. B., Goodbody, A. G., & Pappenberger, F. (2017). Mitigating the impacts of climate nonstationarity on seasonal streamflow predictability in the U.S. southwest. *Geophysical Research Letters*, *44*, 12,208–12,217. https://doi.org/10.1002/2017GL076043

Liguori, G., & Di Lorenzo, E. (2018). Meridional modes and increasing Pacific decadal variability under anthropogenic forcing. *Geophysical Research Letters*, *45*, 983–991. https://doi.org/10.1002/2017GL076548

Luo, J. J., Wang, G., & Dommenget, D. (2018). May common model biases reduce CMIP5's ability to simulate the recent Pacific La Niña-like cooling? *Climate Dynamics*, *50*(3-4), 1335–1351. https://doi.org/10.1007/s00382-017-3688-8

McCabe, G. J., Wolock, D. M., Pederson, G. T., Woodhouse, C. A., & McAfee, S. (2017). Evidence that recent warming is reducing upper Colorado River flows. *Earth Interactions*, *21*(10), 14. https://doi.org/10.1175/EI-D-17-0007.1

Merrifield, A. L., Lehner, F., Deser, C., & Xie, S.-P. (2017). Removing circulation effects to assess central US land-atmosphere interactions in the CESM large ensemble. *Geophysical Research Letters*, *44*, 9938–9946. https://doi.org/10.1002/2017GL074831

Mote, P. W., Hamlet, A. F., Clark, M. P., & Lettenmaier, D. P. (2005). Declining mountain snowpack in western North America. *Bulletin of the American Meteorological Society*, *86*(1), 39–50. https://doi.org/10.1175/BAMS-86-1-39

Newman, A. J., Clark, M. P., Craig, J., Nijssen, B., Wood, A., Gutmann, E., et al. (2015). Gridded ensemble precipitation and temperature estimates for the contiguous United States. *Journal of Hydrometeorology*, *16*(6), 2481–2500. https://doi.org/10.1175/JHM-D-15-0026.1

Okumura, Y. M., DiNezio, P., & Deser, C. (2017). Evolving impacts of multi-year La Niña events on atmospheric circulation and US drought. *Geophysical Research Letters*, *44*, 11,614–11,623. https://doi.org/10.1002/2017GL075034

O'Reilly, C. H., Woollings, T., & Zanna, L. (2017). The dynamical influence of the Atlantic multidecadal oscillation on continental climate. *Journal of Climate*, *30*(18), 7213–7230. https://doi.org/10.1175/JCLI-D-16-0345.1

Park, I.-H., Min, S.-K., Yeh, S.-W., Weller, E., & Kim, S. T. (2017). Attribution of the 2015 record high sea surface temperatures over the central equatorial Pacific and tropical Indian Ocean. *Environmental Research Letters*, *12*(4), 044024. https://doi.org/10.1088/1748-9326/aa678f

Pendergrass, A. G., Knutti, R., Lehner, F., Deser, C., & Sanderson, B. M. (2017). Precipitation variability increases in a warmer climate. *Scientific Reports*, *7*(1), 17966. https://doi.org/10.1038/s41598-017-17966-y

Prein, A. F., Holland, G. J., Rasmussen, R. M., Clark, M. P., & Tye, M. R. (2016). Running dry: The U.S. Southwest's drift into a drier climate state. *Geophysical Research Letters*, *43*, 1272–1279. https://doi.org/10.1002/2015GL066727

Raff, D., Brekke, L., Werner, K., Wood, A., & White, K. (2013). Short-term water management decisions: User needs for improved climate, weather, and hydrologic information (231 pp.). Retreieved from http://www.ccawwg.us/

Rohde, R., Curry, J., Groom, D., Jacobsen, R., Muller, R. A., Perlmutter, S., et al. (2013). Berkeley Earth temperature averaging process. *Geoinformatic Geostatistics An Overv*, *1*, 1–13.

Schmidt, D. F., & Grise, K. M. (2017). The response of local precipitation and sea level pressure to Hadley cell expansion. *Geophysical Research Letters*, *44*, 10,573–10,582. https://doi.org/10.1002/2017GL075380

Schneider, U., Becker, A., Finger, P., Meyer-Christoffer, A., Rudolf, B., & Ziese, M. (2015). GPCC full data reanalysis version 7.0 at 1.0°: Monthly land-surface precipitation from rain-gauges built on GTS-based and historic data.

Schubert, S., Gutzler, D., Wang, H., Dai, A., Delworth, T., Deser, C., et al. (2009). A U.S. Clivar project to assess and compare the responses of global climate models to drought-related SST forcing patterns: Overview and results. *Journal of Climate*, *22*(19), 5251–5272. https://doi.org/10.1175/2009JCLI3060.1

Schubert, S. D., Stewart, R. E., Wang, H., Barlow, M., Berbery, E. H., Cai, W., et al. (2016). Global meteorological drought: A synthesis of current understanding with a focus on SST drivers of precipitation deficits. *Journal of Climate*, *29*(11), 3989–4019. https://doi.org/10.1175/JCLI-D-15-0452.1

Seager, R., Ting, M., Held, I., Kushnir, Y., Lu, J., Vecchi, G., et al. (2007). Model projections of an imminent transition to a more arid climate in southwestern North America. *Science*, *316*(5828), 1181–1184. https://doi.org/10.1126/science. 1139601

Seager, R., Neelin, D., Simpson, I., Liu, H., Henderson, N., Shaw, T., et al. (2014). Dynamical and thermodynamical causes of large-scale changes in the hydrological cycle over North America in response to global warming. *Journal of Climate*, *27*(20), 7921–7948. https://doi.org/10.1175/JCLI-D-14-00153.1

Seager, R., & Henderson, N. (2016). On the role of tropical ocean forcing of the persistent North American west coast ridge of winter 2013/14. *Journal of Climate*, *29*(22), 8027–8049. https://doi.org/10.1175/JCLI-D-16-0145.1

Seager, R., & Hoerling, M. (2014). Atmosphere and ocean origins of North American droughts. *Journal of Climate*, *27*(12), 4581–4606. https://doi.org/10.1175/JCLI-D-13-00329.1

Seager, R., Kushnir, Y., Herweijer, C., Naik, N., & Velez, J. (2005). Modeling of tropical forcing of persistent droughts and pluvials over western North America: 1856–2000. *Journal of Climate*, *18*(19), 4065–4088. https://doi.org/10.1175/JCLI3522.1

Seager, R., & Ting, M. (2017). Decadal drought variability over North America: Mechanisms and predictability. *Current Climate Change Reports*, *3*(2), 141–149. https://doi.org/10.1007/s40641-017-0062-1

Seager, R., & Vecchi, G. A. (2010). Greenhouse warming and the 21st century hydroclimate of southwestern North America. *Proceedings of the National Academy of Sciences*, *107*(50), 21,277–21,282. https://doi.org/10.1073/pnas. 0910856107

Shin, S. I., & Sardeshmukh, P. D. (2011). Critical influence of the pattern of Tropical Ocean warming on remote climate trends. *Climate Dynamics*, *36*(7-8), 1577–1591. https://doi.org/10.1007/s00382-009-0732-3

Simpson, I. R., Seager, R., Ting, M., & Shaw, T. A. (2016). Causes of change in Northern Hemisphere winter meridional winds and regional hydroclimate. *Nature Climate Change*, *6*(1), 65–70. https://doi.org/10.1038/nclimate2783

Smoliak, B. V., Wallace, J. M., Lin, P., & Fu, Q. (2015). Dynamical adjustment of the Northern Hemisphere surface air temperature field: Methodology and application to observations*. *Journal of Climate*, *28*(4), 1613–1629. https://doi.org/10.1175/JCLI-D-14-00111.1

Swain, D. L., Singh, D., Horton, D. E., Mankin, J. S., Ballard, T. C., & Diffenbaugh, N. S. (2017). Remote linkages to anomalous winter atmospheric ridging over the northeastern Pacific. *Journal of Geophysical Research: Atmospheres*, *122*, 12,194–12,209. https://doi.org/10.1002/2017JD026575

Taylor, K. E., Stouffer, R. J., & Meehl, G. a. (2012). An overview of CMIP5 and the experiment design. *Bulletin of the American Meteorological Society*, *93*(4), 485–498. https://doi.org/10.1175/BAMS-D-11-00094.1

Teng, H., & Branstator, G. (2017). Causes of extreme ridges that induce California droughts. *Journal of Climate*, *30*(4), 1477–1492. https://doi.org/10.1175/JCLI-D-16-0524.1

Ting, M., Seager, R., Li, C., Liu, H., & Henderson, H. (2018). Mechanism of future spring drying in the southwest U.S. in CMIP5 models. *Journal of Climate*, *31*(11), 4265–4279. https://doi.org/10.1175/JCLI-D-17-0574.1

Udall, B., & Overpeck, J. (2017). The 21st century Colorado River hot drought and implications for the future. *Water Resources Research*, *53*, 2404–2418. https://doi.org/10.1002/2016WR019638

van Haren, R., van Oldenborgh, G. J., Lenderink, G., Collins, M., & Hazeleger, W. (2013). SST and circulation trend biases cause an underestimation of European precipitation trends. *Climate Dynamics*, *40*(1-2), 1–20. https://doi.org/10.1007/s00382-012-1401-5

Vano, J. A., Das, T., & Lettenmaier, D. P. (2012). Hydrologic sensitivities of Colorado River runoff to changes in precipitation and temperature. *Journal of Hydrometeorology*, *13*(3), 932–949. https://doi.org/10.1175/JHM-D-11-069.1

Wallace, J. M., Fu, Q., Smoliak, B. V., Lin, P., & Johanson, C. M. (2012). Simulated versus observed patterns of warming over the extratropical Northern Hemisphere continents during the cold season. *Proceedings of the National Academy of Sciences of the United States of America*, *109*(36), 14,337–14,342. https://doi.org/10.1073/pnas. 1204875109

Wang, K., Deser, C., Sun, L., & Tomas, R. A. (2018). Fast response of the tropics to an abrupt loss of Arctic sea ice via ocean dynamics. (pp. 1–9). https://doi.org/10.1029/2018GL077325.

Weiss, J. L., Castro, C. L., & Overpeck, J. T. (2009). Distinguishing pronounced droughts in the southwestern United States: Seasonality and effects of warmer temperatures. *Journal of Climate*, *22*(22), 5918–5932. https://doi.org/10.1175/2009JCLI2905.1

Williams, A. P., Seager, R., Abatzoglou, J. T., Cook, B. I., Smerdon, J. E., & Cook, E. R. (2015). Contribution of anthropogenic warming to California drought during 2012–2014. *Geophysical Research Letters*, *42*, 6819–6828. https://doi.org/10.1002/2015GL064924

Woodhouse, C. A., Meko, D. M., MacDonald, G. M., Stahle, D. W., & Cook, E. R. (2010). A 1,200-year perspective of 21st century drought in southwestern North America. *Proceedings of the National Academy of Sciences*, *107*(50), 21,283–21,288. https://doi.org/10.1073/pnas. 0911197107

Woodhouse, C. A., Pederson, G. T., Morino, K., McAfee, S. A., & McCabe, G. J. (2016). Increasing influence of air temperature on upper Colorado River streamflow. *Geophysical Research Letters*, *43*, 2174–2181. https://doi.org/10.1002/2015GL067613

Yeager, S. G., Danabasoglu, G., Rosenbloom, N., Strand, W., Bates, S., Meehl, G., et al. (2018). Predicting near-term changes in the Earth system: A large ensemble of initialized decadal prediction simulations using the Community Earth System Model. *Bulletin of the American Meteorological Society*. BAMS-D-17-0098.1. https://doi.org/10.1175/BAMS-D-17-0098.1

Zhao, S., Deng, Y., & Black, R. X. (2017). Observed and simulated spring and summer dryness in the United States: The impact of the Pacific sea surface temperature and beyond. *Journal of Geophysical Research: Atmospheres*, *122*, 12,713–12,731. https://doi.org/10.1002/2017JD027279